Δελτίο της Ελληνικής Γεωλογικής Εταιρίας τομ. XXXX, 2007
Πρακτικά 11ου Διεθνούς Συνεδρίου, Αθήνα, Μαιος 2007

Bulletin of the Geological Society of Greece vol. XXXX, 2007
Proceedings of the 11th International Congress, Athens, May, 2007

THE ELECTRIC STRUCTURE OF THE SCHIZOSPHERE IN SE THESSALY, GREECE, AND ITS CORRELATION WITH ACTIVE TECTONICS

Tzanis A.[1], and Drosopoulou E.[1]

[1]*Department of Geophysics – Geothermy, University of Athens, atzanis@geol.uoa.gr*

Abstract

We report the results of a magnetotelluric study in SE Thessaly, Greece, and their correlation with the active tectonics of the area. The data comprised 14 wide-band (150-0.005 Hz) soundings performed in the periphery of the cities of Volos, Velestino and N. Anghialos. The spatial analysis of the MT impedance tensor shows a transition from a shallow (< 1 km) geoelectric structure associated with apparent local structural features, to the deeper (> 3 km) schizosphere associated with large scale structures with ESE-WNW to SE –NW orientation. Quantitative interpretation was carried out with 2-D inversion and yielded high quality images of the geoelectric structure at depths 3–15 km; this depth range corresponds to the seismogenic layer. Conductive structures in the general E-W direction could be detected and correlated with neotectonic faults. In addition, a possible relic of the now extinct Mikrothivai volcano (1.5±0.1 Ma BCE) has been identified. Within the seismogenic layer the spatial MT data correlate almost exactly with the stress field calculated by inversion of focal mechanisms from local earthquakes and appear to provide an electrical image of the transition from the dextral NE-SW transformation associated with the N. Aegean trench to approximately N-S extension in the study area.
Key words: *Magnetotellurics, geoelectric structure, stress field inversion, seismotectonics.*

Περίληψη

Παρουσιάζονται τα αποτελέσματα μίας μαγνητοτελλουρικής (MT) μελέτης στην ΝΑ Θεσσαλία, και η συσχέτισή τους με την ενεργό τεκτονική της περιοχής. Τα δεδομένα απαρτίζονται από 14 βαθοσκοπήσεις ευρέος φάσματος (150-0.005 Hz), εκτελεσθείσες στην περιφέρεια των πόλεων Βόλου, Βελεστίνου και Ν. Αγχιάλου. Η χωρική ανάλυση των MT τανυστών δείχνει την ύπαρξη μετάβασης από ρηχή (< 1 km) γεωηλεκτρική δομή προφανώς σχετιζόμενη με τοπικά τεκτονικά χαρακτηριστικά, προς την βαθύτερη (>3 km) σχιζόσφαιρα, η οποία σχετίζεται με δομές μεγάλης κλίμακας και ΑΝΑ-ΔΒΔ έως ΝΑ–ΒΔ προσανατολισμό. Ποσοτική ανάλυση ερμηνεία έλαβε με 2-διάστατη αντιστροφή και απέδωσε υψηλής ποιότητας είδωλα της γεωηλεκτρικής δομής σε βάθη 3–15 km. Αυτό το εύρος βαθών αντιστοιχεί στο σεισμογόνο στρώμα (σχιζόσφαιρα), όπου ανιχνεύθηκαν αγώγιμες δομές με γενικό προσανατολισμό Α-Δ, συσχετιζόμενες με νεοτεκτονικά ρήγματα. Επιπλέον, ανιχνεύθηκε ένα πιθανό υπόλειμμα του εσβεσμμένου πλέον «'ηφαιστείου» των Μικροθηβών (1.5±0.1 Μα). Εντός του σεισμογόνου στρώματος, τα χωρικά MT δεδομένα συσχετίζονται σχεδόν ακριβώς με το πεδίο τάσεων

που προκύπτει από την αντιστροφή μηχανισμών γένεσης τοπικών σεισμών και προσφέρουν ένα γεωηλεκτρικό είδωλο του εντατικού καθεστώτος της περιοχής.
Λέξεις κλειδιά: *Μαγνητοτελλουρική μέθοδος, γεωηλεκτρική δομή, αντιστροφή πεδίου τάσης, σεισμοτεκτονική..*

1. Introduction

Contemporary tectonic processes in SE Thessaly, (22°E – 23.5°E and 39°N – 39.8°N), quite often express themselves in a violent manner. Eight earthquake sequences with main shock magnitude Ms>6 occurred in the area during the present century only (1905, 1911, 1930, 1941, 1954, 1955, 1957 and 1980). Of these, all the post-1954 events occurred within the rectangle 22.5°E – 23.3°E and 39°N – 39.5°N in the periphery of Volos, Velestino and Almyros cities. Apparently, the earthquake hazard of the area is significant and necessitates the thorough understanding of the structures and processes that may be related to the mode of tectonic deformation in the area.

This work reports an effort to contribute in the investigation and comprehension of these tectonic processes with a quantitative study of the upper crustal geoelectric structure, using two-dimensional inversion of magnetotelluric (MT) data and attempting to correlate the results with active tectonic structures and seismological observations.

The reason why observations of the geoelectric structure can image tectonic processes is quite simple. Within the *schizosphere,* (brittle upper crust), faulting generates permeable rock, either directly within the fault zone, (fault gouge, brecia and mylonite), or around it as a result of repeated cycles of loading / unloading and elasto-plastic deformation. The presence of water in the immediate neighbourhood of the fault zone is very important factor for tectonic processes, as it influences creep and/or stability. Around the fault, tectonically induced permeability resulting from micro- and meso-scale fracturing, and crack interconnection is generally aligned with the fault. Healing processes are expected to close the cracks and reduce conductivity, unless they are kept open by continuous accumulation of deformation, either seismic or aseismic. Moreover, the more extensive and pervasive the microfracturing, (more heavily deformed the material), the more conductive the rock may be. Cracks may also form beneath the schizosphere, in the brittle-plastic transition; *cataclastic flow* is typical in this stress regime. At these depths deformation occurs concurrently with low grade metamorphism involving liquid phase (brines), which may increase the electrical conductivity when interconnected – brines are important fluid phases in metamorphic rocks and were actually found in the deep upper crust by the Kola borehole (e.g. Kozlovsky 1988) as well as the German Continental Deep Borehole (KTB) at the Schwartzwald.

It should be noted that there have been two previous attempts to study the crustal geoelectric structure of SE Thessaly by Tzanis et al (1994a, b). However, they were both based on a primarily qualitative analysis of the MT observations and a critical analysis of seismological data. The 1-D quantitative interpretation (one-dimensional inversion) employed in these studies was clearly insufficient to provide adequate images of geoelectric structures, let alone facilitate their correlation with active faulting; in retrospective, it has actually overestimated the penetration depth of the MT data. The present study is using a state-of-the-art 2-D inversion algorithm, which allows the reconstruction of detailed and interpretable images of geoelectric structures with lateral resistivity variations.

2. Geotectonics and Seismicity

The contemporary tectonic setting of SE Thessaly began taking shape during the Pliocene. A dominantly NE-SW extensional stress field controlled the tectonic deformation until the Early Pleistocene, (e.g. Caputo and Pavlides 1993), forming a conjugate system of normal faults with general directions NW-SE and NE-SW and resulting in the formation of NW-SE trending basins, including the tectonic depression of Almyros basin – Pagasitikos gulf, which remained active

through the Quaternary. Traces left by this tectonic episode on the surface of SE Thessaly can clearly be seen in the lineaments of Figure. 1 (left), drawn from observations of LANDSAT images (Polyzos 1977, Kronberg and Guenther 1977).

A younger phase of tectonic activity began in the Middle Pleistocene and continues until the present. Based on focal mechanism analysis of major earthquakes, Drakopoulos and Delibasis (1982) also proposed that the main stress field has an approximately N-S direction (actually NNE-SSW) and the resulting normal faults an approximate E-W strike. Taymaz *et al.* (1991) concur with this idea and Papazachos *et al.* (1983) argue for a NNW-SSE extensional field. A detailed geotectonic study of the Volos-Almyros area with analysis of satellite images, aerial photography and surface observations (Cratchley 1983) revealed a tectonic fabric dominated by fault structures with directions NE-SW (N50°-N60°), ENE-WSW (approx. N80°) and NW-SE (N100°-N130°). In most cases, these fault zones correspond with morphological and morphotectonic characteristics of the area. The tectonic direction N80° (as for instance is the recently activated Nea Anghialos fault zone), is known to be generated by contemporary deformation processes, while the direction N50°-N60° may represent older (Pliocene) tectonic episodes. The direction (N100°-N130°) is rarely mentioned in existing literature as a major fault zone and its significance is still unknown. Caputo (1990) and Caputo and Pavlides (1993) assign a lesser, or no significance to these tectonic lineaments at longitudes east of approximately 22.6°E, but they illustrate them as dominant features to the west of 22.6°E. The same authors discuss of deformation in terms of geological and tectonic arguments for an approximately N-S extensional field.

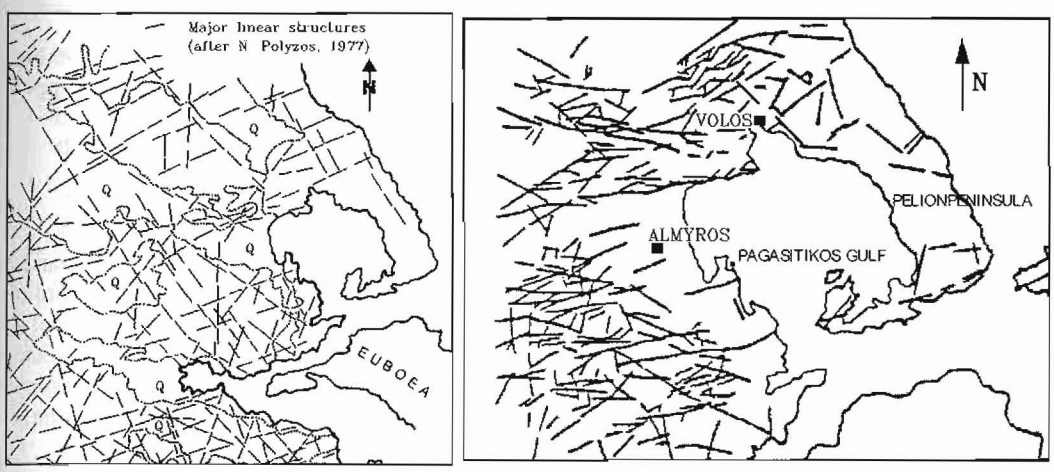

Figure 1 – Left: Lineaments from the Pliocene tectonic episodes, as traced from LANDSAT images (after Polyzos 1977) ; Q denotes the Quaternary basins. Right: The tectonic analysis of Cratehley (1983)

On the basis of a critical analysis of qualitative MT and seismotectonic observations, Tzanis *et al.* (1994b) argue for a geotectonic model involving homogeneous deformation by shearing in two conjugate planes forming a 30° angle (moderate-high internal friction). The configuration of the stress field is such that the E-W plane experiences almost pure N-S extension and expresses normal faulting with a small dextral component, while the NW-SE plane absorbs most of the horizontal compressive stress and expresses normal, oblique-slip faulting with sinistral slip. In this way, the entire system experiences dextral block rotation about the vertical axis, but little or no mass translation. This model has certain differences, but produces the same effect with the block model of distributed deformation by faulting, proposed by McKenzie and Jackson (1986).

To the south of Almyros basin, only two tectonic directions are apparent. The first strikes approximately at N80° and may be correlated with the same contemporary tectonic processes, which generate N.Anghialos fault zone. The second strikes at N100°-N130° and according to Mariolakos

and Papanikolaou (1987), it defines the bonndary of a tectonic dipole. It may be possible to correlate these tectonic lineaments with the corresponding directions observed to the north of Almyros basin, but conclusive results have not been given as yet.

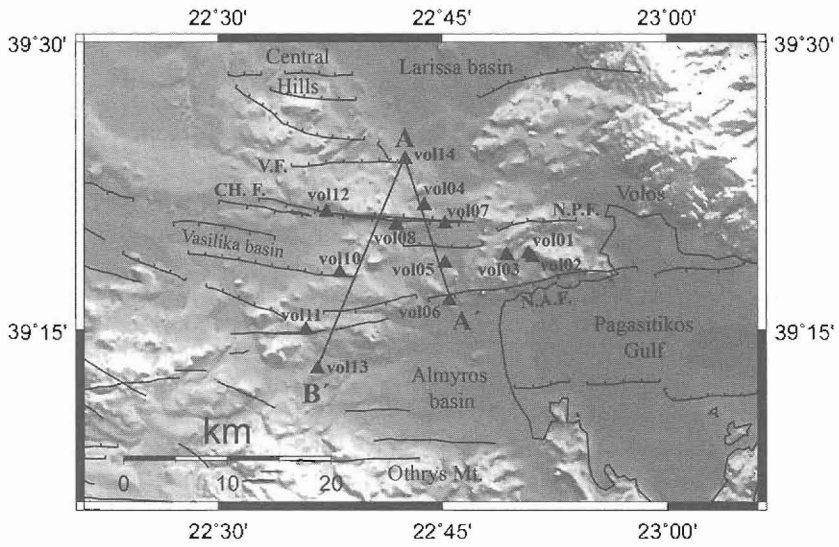

Figure 2 – Map of the study area (SE Thessaly) illustrating the measurement sites and the transects along which 2-D inversion was carried out. The major neotectonic faults mapped by Caputo and Pavlides (1993) are also overlaid: N.A.F – Nea Anghialos Fault; CH.F – Chalkodonio or *Rigaio* Fault; N.P.F. – Neai Pagassai Fault; V.F. – Velestino Fault

3. Magnetotelluric Data Analysis and Results

The magnetotelluric (MT) data was acquired in two phases, during the summer of 1992 (Tzanis *et al.* 1994) and the autumn of 1994, providing a total of 13 soundings (Fig. 2). Fairly standard observation procedures were followed, leading to the acquisition of five cartesian components of the natural EM field over the nominal frequency bandwidth 150-0.005 Hz. Data quality was sufficient for standard processing techniques, (e.g. Sims *et al.* 1971) to provide satisfactory Earth response functions with low levels of uncertainty. Rigorous testing (e.g. Bahr 1988), has confirmed the absence of galvanic distortion from the data.

3.1. Spatial analysis and the configuration of the geoelectric structure

This exercise endeavours to extract information about the configuration of the induced natural EM fields, which, in turn, depend on the geometry and confignration of lateral inhomogeneities in the geoelectric structure. The method of spatial analysis used herein is the Canonical Decomposition of Yee and Paulson (1986), which provides as a function of frequency, the magnitude, phase, azimuth and ellipticity of the maximum and minimum characteristic states of the impedance tensor, respectively described by the relationships $E(\omega,\Theta_E,\Phi_E) = \mu_1(\omega)H(\omega,\Theta_H,\Phi_H+\pi/2)$ and $E(\omega,\Theta_E,\Phi_E+\pi/2) = \mu_2(\omega)H(\omega,\Theta_H,\Phi_H)$; Φ is the azimuthal directiou of the electric/magnetic fields and is associated with the strike of the geoelectric structure; $\tan(\Theta)$ is the ellipticity. More specifically, $E(\omega,\Theta_E, \Phi_E)$ and $E(\omega,\Theta_E,\Phi_E+\pi/2)$ respectively represent the maximum and minimum electric field at the angular frequency ω, along the directions Φ_E and $\Phi_E+\pi/2$; $\mu_1(\omega) > \mu_2(\omega)$ are the complex maximum and minimum impedances along the directions Φ_E and $\Phi_E+\pi/2$; finally, $H(\omega,\Theta_H,\Phi_H)$ and $H(\omega,\Theta_H,\Phi_H+\pi/2)$ respectively represent the maximum and minimum magnetic field along the directions Φ_H and $\Phi_H+\pi/2$. In the case of 2-D geoelectric structures, $\Phi_E=\Phi_H$ and $\Theta_E=\Theta_H=0$. In 3-D structures however, one should rather observe $\Phi_E\neq\Phi_H$ and $\Theta_E\neq\Theta_H\neq0$. It is not straightforward to see in this thrifty presentation, but the essence of this analysis is that it ap-

proaches the geoelectric structure as the equivalent of a birefringent material at low frequencies and large scales. In this context, there is a fast (resistive) direction, which on the horizontal plane is defined by (μ_1, Φ_E, $\Phi_H+\pi/2$), and a slow (conductive) direction defined by (μ_2, $\Phi_E+\pi/2$, Φ_H).

An example of the Canonical Decomposition applied to the data of Site vol07 is provided in Figure 3; it is *typical* of the survey and may simultaneously serve as a demonstration of the quality and properties of the data. A first and important observation regards the absence of static shifts: the maximum and minimum apparent resistivities can be seen to converge at high frequencies. The response exhibits multi-dimensional characteristics and is clearly indicative of a significant nearby resistivity inhomogeneity. A very important feature is the rotation of the strike (azimuthal angles) from approx. NNW-SSW at periods shorter than 2-5s, to NW-Se at periods longer than 10s. This rotation is also *typical* of the entire survey and may be attributed to a corresponding rotation of the geoelectric principal directions (strike) from local to regional (see ensuing discussion). The local structure is almost two-dimensional ($\Phi_E \approx \Phi_H$, small ellipticities). The transition to the regional structure comprises a 3-D effect, responsible for the deviating azimuthal angles and significant ellipticities. Due to the diffusive nature of the natural induction process, the wake of the effect spreads over a relatively broad period spectrum, diminishing toward the longer periods (vanishing ellipticities). The latter indicates that the regional structure is also quasi-2D and can therefore be interpreted with two-dimensional analysis tools.

Now, that on assuming (quasi) two-dimensional local and regional structures, the spatial analysis of the impedance tensor boils down to the following simple rules (see also Swift1971):

- On the conductive side of a 2-D interface, the maximum electric field (maximum state) will be parallel to the strike and will correspond to the Transverse Electric (TE) mode of EM field propagation.

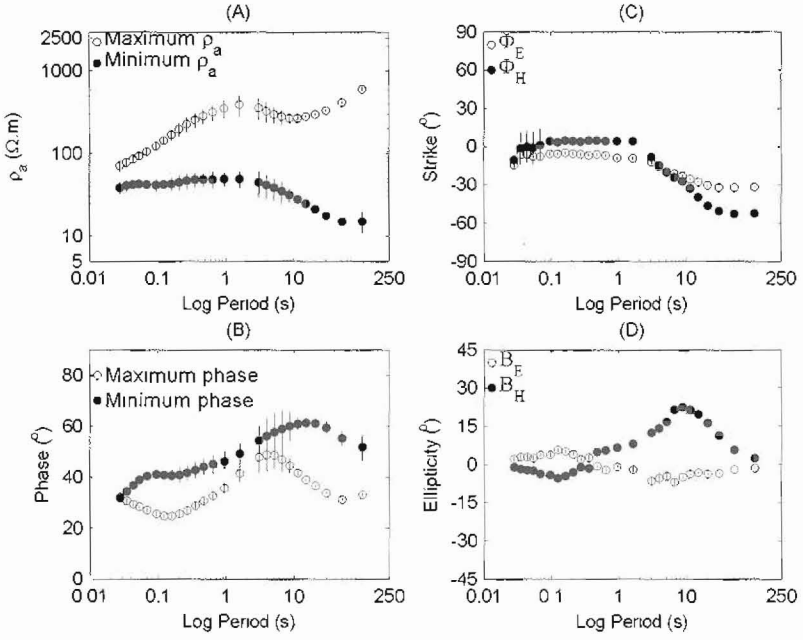

Figure 3 – A *typical* example of the magnetotelluric data obtained in the study area: The Canonical Decomposition of the impedance tensor at Site vol07

- On the resistive side of a 2-D interface, the maximum electric field will be normal to the strike and will correspond to the Transverse Magnetic (TM) mode of EM field propagation.

Let us again note that in the case of 3-D structures, because $\Phi_E \neq \Phi_H$, these rules must be applied with caution and always bearing in mind the magnitude of the skew angle ($\Phi_E - \Phi_H$) and the ellipticity ($\tan\Theta_E$, $\tan\Theta_H$), which are ample indicators of the strength of the 3-D effects.

After due consideration of the information afforded by the Canonical Decomposition, (as per Fig. 3), we conclude to the following: **(a)** To study purely local and near surface structures we use the frequency band 150-30 Hz (0.0066–0.33 s); as it turns out, this band probes depths down to approximately 500-1000 m at most (see Section 3.2). **(b)** To study regional structures we use the frequency band 0.1-0.005 Hz (10-100s), which turns out to probe the entire local section of the schizosphere at depths below 2-3 km (also see Section 3.2).

The higher frequencies (Fig. 4, 150-30 Hz,) respond to dominantly 2-D structures, as attested to by the very low ellipticities. Due to the local nature of the response in this frequency band, the study area may be subdivided into 3 geoelectric sectors. In the *east* sector (sites vol01-vol03), the nearly orthogonal maximum impedance states between sites vol02 and vol03 are consistent with the assumption of a geoelectric interface with orientation WNW-ESE to NW-SE, possibly related to a fault zone (i.e. a *de facto* conductor); in this case, site vol03 would appear to respond in the TM mode over the resistive side, and sites vol01 and vol02 in the TE mode over the conductive side of the interface. The *west* sector comprises sites vol8-vol13 and may be further separated into a northern (sites vol08, vol10 and vol12), and a southern (vol11 and vol13) domain. In the northern domain, NNE-SSW to NNW-SSE orientations of the impedance maximum state are observed, consistent with TM mode response above the resistive side of WSW-ENE to WNW-ESE oriented geoelectric interfaces. In the southern domain the maximum impedance orientation is N-S at site vol13 and E-W at site vol11. This is compatible with the existence of an E-W conductor in the immediate vicinity of site vol11 and possibly beneath it; owing to its location, this conductor may be related with a fault zone comprising the westward extension of N. Anghialos fault. The *central* sector comprises soundings vol04-vol07 and vol14. The maximum impedance state has NNW-SSE directions, also compatible with response to TM mode above the resistive sides of WSW-ENE interfaces. The maximum electric field direction changes to NW-SE at the north of the sector (site vol14) presumably responding to the structures of the massive Larissa basin, which has an identical orientation.

At the lower frequency band (Fig. 5, 0.1-0.005 Hz), the geoelectric structure exhibits a non-negligible 3-D component at the west and central sectors (significant ellipticities). However, the remarkable observation is a swift change in both its spatial and quantitative characteristics (see Fig. 3). Specifically, the general orientation of the impedance maximum state at sites vol1 – vol10 and vol12 is NW-SE to NNW-SSE. On the other hand, at the two southernmost sites (vol11 and vol13) the maximum states exhibit N-S to NNE-SSW orientations. The interpretation of these observations is not straightforward, partly because of the relatively small number and the geographical distribution of the observations. However, note that sites vol11 and vol13 are located at the south margin of the investigated area. The significant difference of the qualitative characteristics between these two sites and the other eleven may signify the existence of a structural block with particular geoelectric properties, embedded between the structural units of Larissa basin – Central Highlands – Karditsa basin to the north and Almyros basin to the south. This block will henceforth be referred to as *the Chalkodonio block* and within it, the impedance maximum state appears oriented at very high angles with respect to neotectonic faulting structures, such as are the N. Anghialos, Chalkodonio and Velestino faults (i.e. *de facto* conductive zones with an average E-W orientation). If this interpretation is correct, MT measurements on the Chalkodonio block indicate that the principal mode of induction at depths greater than 2-3 km b.m.s.l. could be approximated with a TM mode response to large scale, NE-SW to ENE-WSW geoelectric structural units.

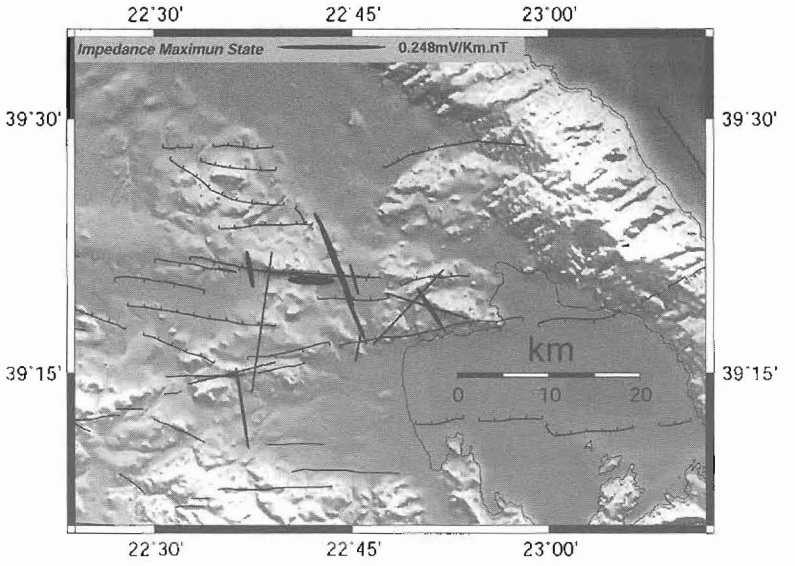

Figure 4 – The maximum characteristic states of the electric field (maximnm impedance), averaged over the frequency band 150 – 30 Hz

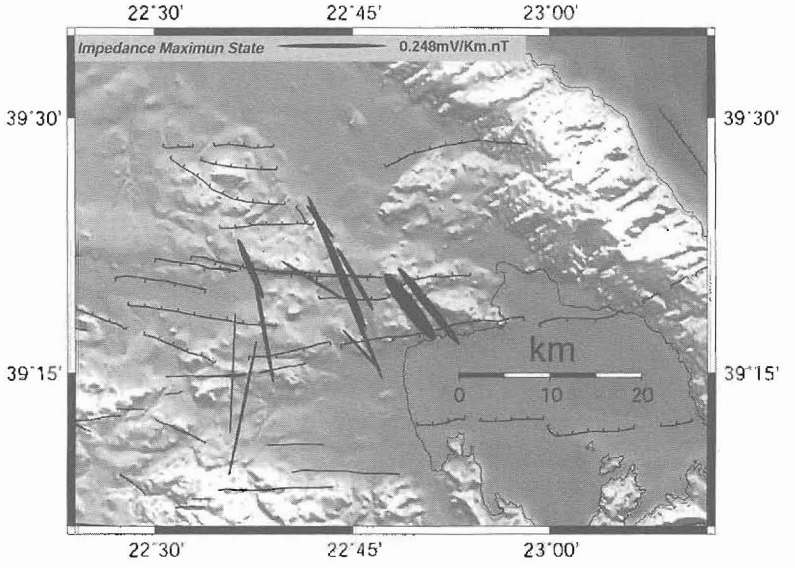

Figure 5 – The maximum characteristic states of the electric field (maximum impedance) averaged over the frequency band 0.1 – 0.005 Hz

3.2. Quantitative analysis – 2-D Magnetotelluric Inversion

Two-dimensional inversion has been carried out along the transects A-A′ and A-B′ (Fig. 2) with the algorithm of Rodi and Mackie (2001). Only frequencies *lower* than 2-4 Hz were used in the inversion; this was mandatory, because the density of measurements along transects does not allow adequate resolution of local/ shallow interfaces with any degree of confidence. In consequence, the investigation focused on the deeper geoelectric structure assuming that the maximum impedance state represents induction in the TM mode, as concluded by the spatial analysis above. In all cases, a discretized homogenous half-space was used as a starting model; the discretization scheme is apparent in Figures 7 and 8. Topography was also taken into consideration. Several inversions with different regularization factors were carried out before a final model was declared. The shallow

part of the structure reconstructed from these inversions will not be discussed because it is insufficiently constrained as explained above.

A typical example of the results is shown in Figure 6, which compares the observed (discrete lines) and fitted response (continuous and dashed lines, final model) at Site vol07. The excellent quality of the final models is also evident in the χ^2 misfit: For Transect A-A′ this is χ^2=86.3, with an expected value of 192. For transect B-B′ this is χ^2=89.5 with an expected value of 260.

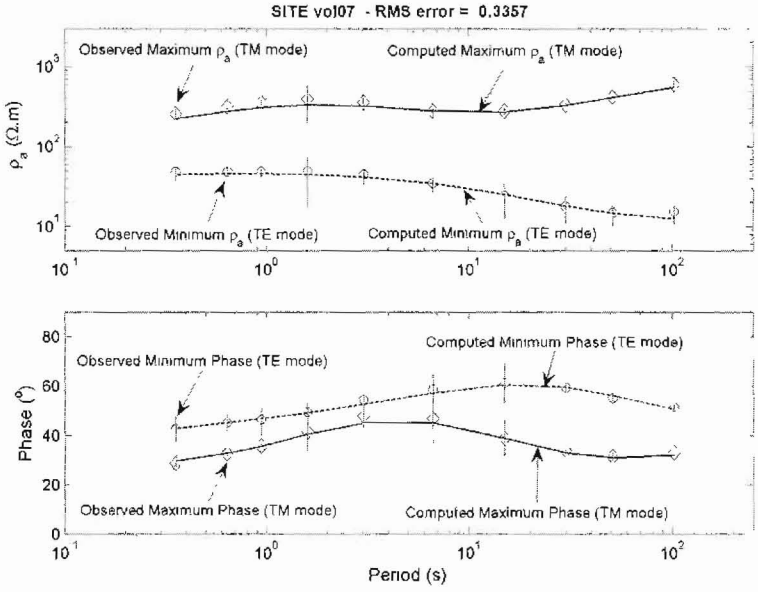

Figure 6 – Observed and modelled (inverted) response at Site vol07. The maximum state corresponds to the TM mode and the minimum state to the TE mode, as indicated by the spatial analysis (see Fig. 5)

Figure 7 illustrates the image of the geoelectric structure along Transect A-A′. The downward projection of the neotectonic normal faults mapped by Caputo and Pavlides (1993) is also illustrated. This was actually made by draftsman's licence and due consideration of the curvature (listration) expected of normal faults. This transect is characterized by high resistivity contrasts, the most prominent being a very good conductor between sites vol05 and vol07 (1 – 10 Ωm, designated as #2a). This conductor also has significant depth extent, from approximately 2 km, to at least 14 km. More importantly, it is located right on the expected trajectory of the Chalkodonio fault which, thus, appears to contribute in its formation. Caputo and Pavlides (1993) have mapped a nameless local fault (?) which appears to be antithetic to Chalkodonio fault. There's no individual geoelectric signature of this feature. The N. Anghialos fault is important, but is located at the very southern margin of transect and cannot be imaged with this data set. However, it does seem to be associated with relatively low resistivities (ca. 20-50 Ωm). Finally, due to its location at the very northern end of the section, the good conductor observed at depths 3 – 6 km beneath and to the north of site vol14, cannot be interpreted with confidence. It appears at the margin of the Larissa basin and may be part of the deeper structure of this tectonic unit – the action of neotectonic faults, such as the Velestino fault, may have affected its evolution, but sound and conclusive statements cannot be made without additional data.

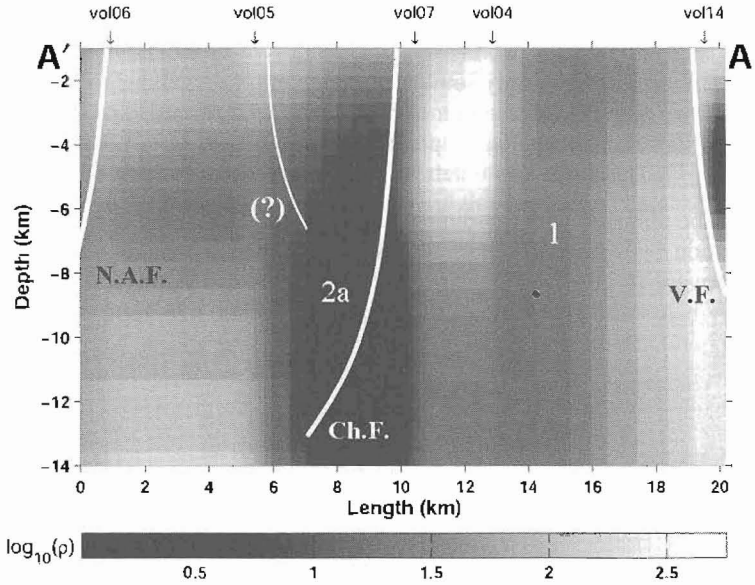

Figure 7 – Geoelectric image of the schizosphere along transect A-A′, obtained by two-dimensional inversion. Depths refer to mean sea level. The numbers indicate conductors correlated between transect A-A′ and A-B′ (also see Fig. 7)

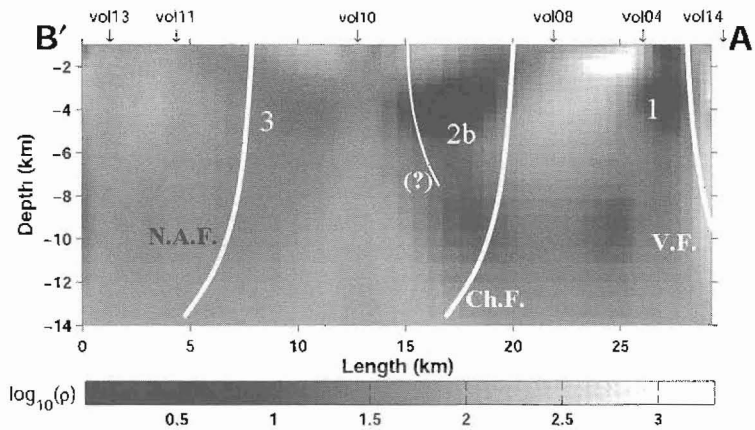

Figure 8 – Geoelectric image of the schizosphere along transect A-B′, obtained from two-dimensional inversion. Depths refer to m.s.l. The outline numbers indicate conductors correlated between transects A-A′ and B-B′ (see also Fig. 7)

Figure 8 illustrates the image of the geoelectric structure along Transect A-B′, together with the projection of the neotectonic normal faults mapped by Caputo and Pavlides (1993). Significant conductive structures in this section appear between sites vol10 and vol08 (1 – 15 Ωm). Between sites vol10 and vol08 these structures, designated with #2b, correlate with the location of Chalkodonio and (?) faults, albeit not as clearly as in Transect A-A′, but sufficiently enough, as to suggest a causal relationship. The apparent trajectory of N. Anghialos fault passes through a broad, relatively conductive zone, (30 – 100 Ωm , designated with #3), which does not have any outstanding characteristic. Note, however, that the geoelectric image at this area is a necessarily low resolution one, due to the relatively long separation between sites vol10 and vol11. On the other hand, site vol11 is located very near the trace of the fanlt and should have detected the presence of a good conductor, had one been there at all. In consequence, we are inclined to interpret this zone

in terms of the conductive halo formed around the fault. Finally, the conductive feature observed at depths of 1-8 km to the nortb of site vol04 and designated as #1, is the same with the corresponding feature of Transect A-A′, only somewhat differently imaged due to different parameterization between the two transects. Inasmuch as it cannot be correlated directly with any mapped neotectonic feature, its origin is uncertain; perhaps it may be traced to older (e.g. Pliocene) tectonic episodes.

Further insight can be obtained with a 3-dimensional presentation of the two transects, as per Figure 9. The correlation between conductors #2 and their apparent link with Chalkodonio and (?) faults is straightforward to observe. Their main difference is that conductor #2a has great depth extent – apparently below the penetration of this data set – while #2b appears confined to the upper crust (schizosphere). There's no easy explanation of this observation. Note however, tbat Transect A-A′ traverses the (now extinct) volcanic area, at which the Microthivai basalts had erupted ca. 1.5 Ma BCE. Noting that the extrusion of mafic rocks directly from the lower crust/ mantle implies a very significant tectonic episode that must have ruptured through the entire lithosphere, it is conceivable that remnants of this episode, rejuvenated by neotectonic activity and endowed with the capacity of hosting water may explain this deep reaching geoelectric feature. Traces of conductive structure possibly associated with N. Anghialos fault, appear only in transect B-B′ (#3).

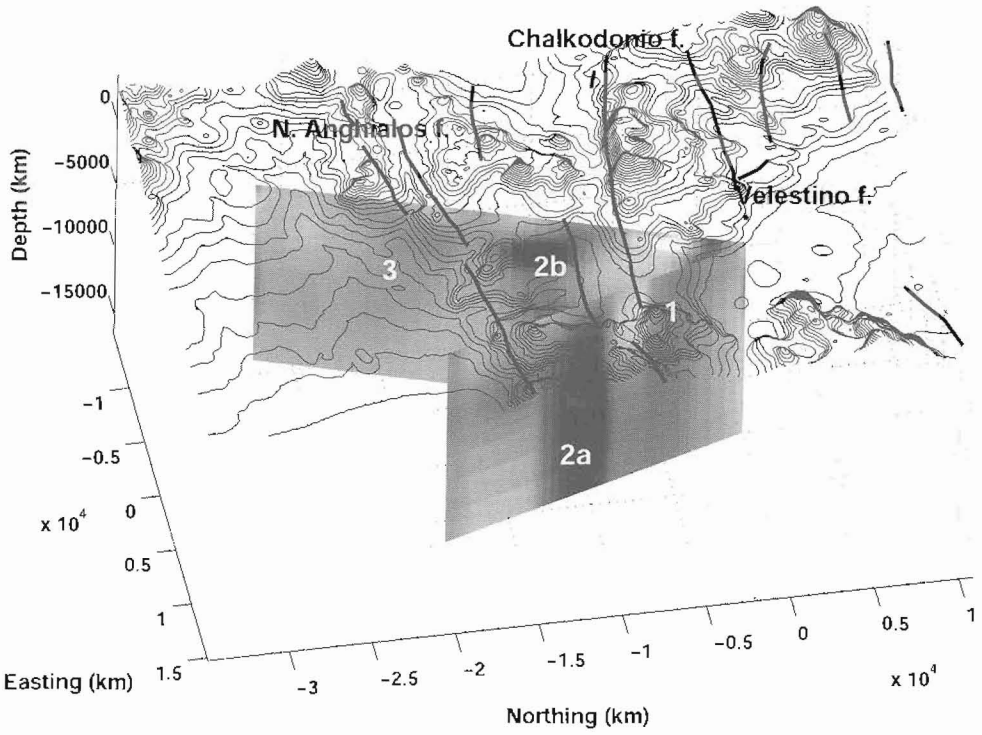

Figure 9 – Composite 3-dimensional representation of transects A-A′, and B-B′, with topography and the neotectonic faults mapped by Caputo and Pavlides (1993). Perspective projection from east to west

4. Discussion and Conclusions

The spatial analysis of the MT impedance tensor shows a transition from a shallow (< 1 km) geoelectric structure exhibiting local characteristics that are usually associated with apparent local structural features, to the deeper (> 2 km b.m.s.l.) upper crust associated with large scale processes

and structures with ESE-WNW to SE –NW orientation. On the basis of this analysis, quantitative interpretation was carried out with 2-D inversion and yielded high quality images of the geoelectric structure at depths 2 – 15 km. Conductive structures in the general E-W direction could be detected and correlated with the Chalkodonio neotectonic fault (notably the purported source of the 1957 earthquake sequence, Caputo 1990). The other known important fault in the area, N. Anghialos fault, could not be imaged at the same level of detail due to the geographical distribution of MT measurements; only of the conductive halo around the fault could be observed in one transect (B-B′). In addition to these features, a possible conductive relic of the now extinct Mikrothivai volcano (1.5±0.1 Ma BCE) has been identified.

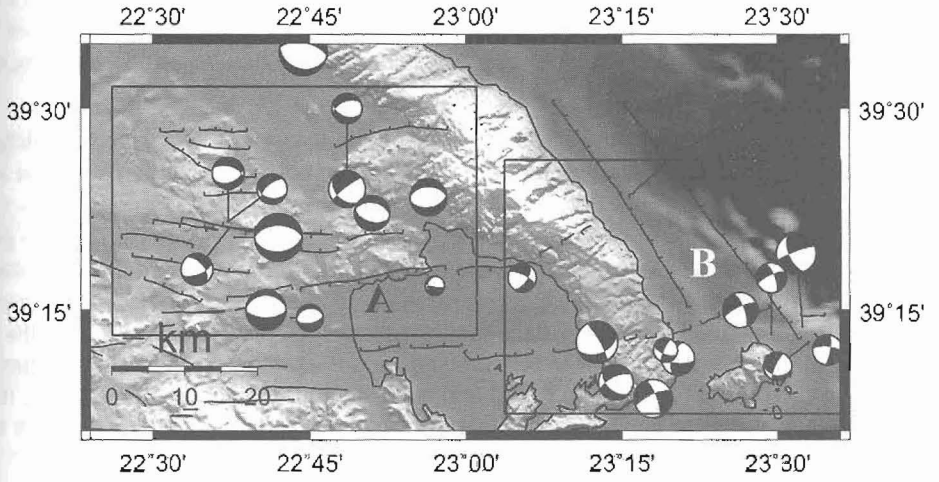

Figure 10 – Locations and focal mechanisms of local earthquakes (Hatzfeld *et al.* 2001)

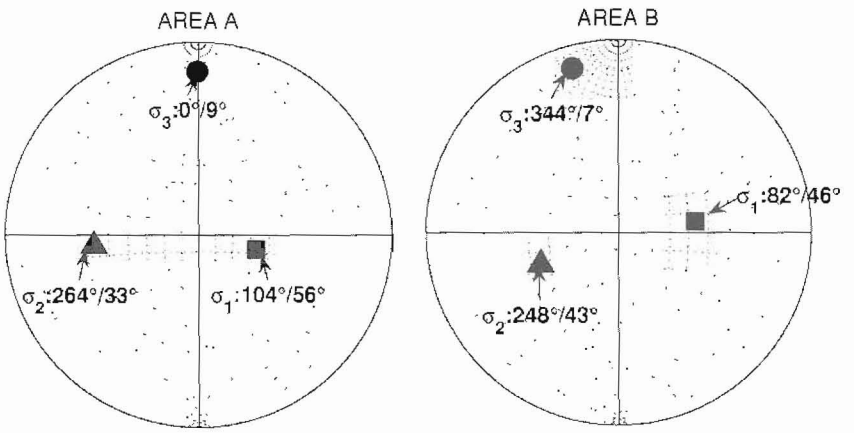

Figure 11 – The stress field derived from the focal mechanisms of Figure 10, using Michael's (1984, 1987). Left: Area A of Figure 10. Right: Area B of Figure 10. Wulff projection

Now, consider that the MT data used in the inversions (frequencies 5–0.005 Hz, depths 3–15 km,) in effect image the seismogenic layer, in which the contemporary active tectonics is expressed. The geoelectric trend of this layer is generally ESE-WNW. This observation deserves additional scrutiny. One path of inquiry is to study the stress field by inverting focal mechanism data from small earthquakes, which encode information about the background deformation mode.

The only source of focal mechanism data from local earthquakes is Hatzfeld *et al.* (2001). Herein, use was made of quality A and B solutions, according to these author's criteria. The locations and

focal mechanisms of those earthquakes used for stress inversion are shown in Figure 10. Based on their general characteristics, two regions with apparently different type of faulting were identified: Area A comprising the Chalkodonio block with predominantly normal faulting and Area B comprising Mt. Pelion and the Sporhades area (western terminus of the N. Aegean trench) with predominantly oblique-slip faulting.

Stress inversion was performed with the method of Michael (1984, 1987). Figure 11 shows the results. In Area B (right) the σ_1-σ_3 plane (P-T plane) is oriented NE-SW and the stress field is expected to generate dextral, normal to oblique-slip faults in the NW-SE direction, consistent with expectation for the N. Aegean Trench, whose influence appears to dominate the tectonics of that area. In Area A (left) the σ_1-σ_3 plane is NNE-SSW (clockwise rotation of the order of 15°–20° with respect to area B) and the stress field more extensional in character, but it still allows for a smaller horizontal slip component, which in southerly and northerly dipping faults should be right-lateral.

Now, observe that at the depths of the seismogenic layer, the maximum impedance orientation is parallel to the σ_1-σ_3 plane: At the east sector of the Chalkodonio block it is almost identical to the σ_1-σ_3 plane direction of Area B, while at the central and western sectors, it appears to rotate clockwise and be more like the σ_1-σ_3 plane direction of Area A (see Fig. 5). Because faults generally develop at high angles, or perpendicular to the σ_1-σ_3 plane and define longitudinal conductive zones, while rock formations in between are comparatively resistive, the TM mode response encoded in the MT data should be approximately parallel to the σ_1-σ_3 plane. As it turns out, the electromagnetic and earthqnake data appear to be telling *one and the same* story: The shcizosphere trying to cope with the changes in the stress field and main faulting directions. Remarkably, in this case, the electromagnetic data emerge as an effective indicator of the configuration of the stress field!

As a final comment, note that there's an arguably simple physical basis to establish a relationship between EM induction and deformation processes in active domains. As shown here, the MT data can provide valuable information on the modes of active tectonics and their joint (associative) interpretation with seismotectonic data can be a very nseful tool in geotectonic analysis (for a more detailed discussion see Tzanis and Makropoulos 1999). Although seismotectonic data afford a direct observation of active faulting processes, reliable seismicity records and focal mechanisms exist only for the later decades of the 20th century. Earthquakes however, may nucleate in any fanlt within an active seismic zone and only a portion of the seismogenic faults have been activated during this period. It follows that the correlation of reliable seismotectonic and electromagnetic data over the broader tectonic zone may provide an indication of the extent of active faulting systems, hence the seismogenic potential of a given area.

5. Acknowledgments

The acquisition and analysis of the magnetotelluric data was supported by the European Commission under contracts EPOC-CT91-0045 and EV5V-CT94-0499.

6. References

Bahr, K., 1988. Interpretation of the magnetotelluric impedance tensor: regional induction and local telluric distortion, *J. Geophys.*, 62, 119-127.

Caputo, R., and Pavlides, S., 1993. Late Cainozoic geodynamic evolution of Thessaly and surroundings (central – northern Greece), *Tectonophysics,* 223, 339-362.

Caputo, R., 1990, Geological and Structural Study of the Recent Active and Brittle Deformation of the Neogene - Quaternaty Basins of Thessaly (Central Greece), *PhD Thesis*, University of Thessaloniki.

Cratchley, C.R., 1983. Volos Project, PA 85F. Progress report, IGS component for the period 1st April-30 September 1983, *British Geological Survey*.

Drakopoulos, J., and Delibasis, N., 1982. The focal mechnanism of earthquakes in the major area of Greece for the period 1947-1981, Univ. of Athens, *Seismological Laboratory Publication* No 2, 185pp.

Hatzfeld, D., Ziazia, M., Kementzetzidou, D., Hatzidimitriou, P., Panagiotopoulos, D., Makropoulos, K., Papadimitriou, P., and Deschamps, A., 1999. Microseismicity and focal mechanisms at the western termination of the north Anatolian Fault and their implications for continental tectonics, *Geophys. J. Int.,* 137, 891-908

Kozlovsky, Ye.A., 1984. The world's deepest well, *Scientific American*, 251, 106-112.

Kronberg, P., and Guenther, R., 1977. Fracture patterns and principles of crustal fracturing in the Aegean region, *Proc. VI Colloquium on the geology of the Aegean region*, II, Athens 1977.

Mariolakos, E., and Papanikolaon, D., 1987. Είδος παραμόρφωσης και σχέση παραμόρφωσης – σεισμικότητας στο Ελληνικό Τόξο, *Bull. Geol. Soc Greece,* XIX, 59-76.

McKenzie, D., and Jackson, J.A., 1986. A block model of distributed deformation by faulting, *J. Geol. Soc. Lon.,* 143, 349-353.

Michael, A. J., 1984. Determination of stress from slip data: Faults and folds, *J. Geophys. Res.*, 89, 11517-11526.

Michael, A. J., 1987. Use of focal mechanisms to determine stress: A control study, *J. Geophys. Res.*, 92, 357-368.

Papazachos, B.C., Panagiotoponlos, D.G., Tsapanos, T.M., Mountrakis, D.M., and Dimopoulos, G.Ch, 1983. A study of the 1980 summer seismic sequence in Magnesia region of Central Greece, *Geophys. J. R. astr. Soc.*, 75, 155-168.

Polyzos, N., 1977. Untersuchungen zur geologischen Auswertbarkeit von Satelitenaufnahmen am Beispiel Mittelgriechenlands, *Thesis*, Geolog. Institut, Tech. Univ. Claustahl.

Rodi, W., and Mackie, R.L., 2001. Nonlinear conjugate gradients algorithm for 2-D magnetotelluric inversion, *Geophysics*, 66 (1), 174–187.

Scholz, C.H., 1990. *The Mechanics of Earthquakes and Faulting*, Cambridge University Press.

Sims, W.S., Bostick, F.X., Jr., and Smith, H.W., 1971. The estimation of magnetotelluric impedance tensor elements from measured data, *Geophysics,* 36, 938-942.

Swift, C. M., 1971. Theoretical magnetotelluric and TURAM response from two-dimensional inhomogeneities, *Geophysics*, 36, 38-52.

Taymaz, T., Jackson, J.A., and McKenzie, D., 1991. Active tectonics of the north and central Aegean Sea, *Geophys. J. Int*, 106, 433-490.

Tzanis, A., and Makropoulos, K., 1999. Magnetotellurics and seismotectonics in the analysis of active domains: An essential Combination? *Phys. Chem. Earth (A),* 24 (9), 841-847.

Tzanis, A., Makropoulos, K., Martin, J-L., Cormy, G., and Drakopoulos, I., 1994a. Contribution to the study of tectonic deformation in south-east Thessaly, Greece: Geomagnetic deep sounding and seismotectonic observations. *Proceedings, 2nd Congress of the Hellenic Geophys. Union*, vol 2, 733-748 Florina, Greece, 5-7 May 1993.

Tzanis, A., Ziazia, M., Kementzetzidou, D., and Makropoulos, K., 1994b. A model of contemporary tectonics in SE Thessaly, Greece, as derived from magnetotelluric, GDS and Seis-

motectonic investigations. *Proceedings, XXIV ESC Gen. Assembly,* Athens, Greece, 1994, Vol. I, 419-431.

Yee, E., and Paulson, K.V., 1987. The Canonical decomposition and its relationship to other forms of magnetotelluric impedance tensor analysis, *J. Geophys.*, 61, 173–189.